The absolute double-differential Compton scattering cross section of Cu 1s electrons

1996 J. Phys.: Condens. Matter 8 2153

(http://iopscience.iop.org/0953-8984/8/13/007)

J. Phys.: Condens. Matter **8** (1996) 2153–2162. Printed in the UK

The absolute double-differential Compton scattering cross section of Cu 1s electrons

J Laukkanen, K Hämäläinen and S Manninen

Department of Physics, PO Box 9, FIN-00014, University of Helsinki, Finland

Received 2 November 1995, in final form 22 January 1996

Abstract. The absolute double-differential Compton scattering cross section for high-energy x-rays has been measured for K-shell electrons of copper using the coincidence technique. Three different momentum-transfer values have been used which are all in the interesting range where the role of the electron binding energy is important. The results have been compared with the existing calculations emphasizing the role of the impulse approximation. The impulse approximation is found to work surprisingly well and the small deviations are explained via more detailed calculations.

1. Introduction

Inelastic scattering of high-energy photons is a widely adopted technique for studying the ground and the excited electron states. In the Compton scattering regime (large momentum transfer) it is assumed that the electron binding energies are small compared with the energy transferred in the scattering process. In this case the cross section only depends on the ground-state wave functions. This so-called impulse approximation (IA) [1] has been extremely useful when the experimental results have been compared with the theory. This is mainly related to the fact that a quantity, the so-called Compton profile $J(p_z)$, which is defined by

$$J(p_z) = \int\int n(\boldsymbol{p})\ \mathrm{d}p_x\ \mathrm{d}p_y \tag{1}$$

where $n(\boldsymbol{p})$ is the ground-state momentum density, can be factorized from the inelastic scattering cross section. This opens up a direct way of comparing the experimental data and the wave-function calculations. It should noticed, however, that the Compton scattering experiment gives only the one-dimensional projection of the momentum density onto the direction of the scattering vector (p_z) while it is averaged over the other two dimensions (p_x and p_y).

When the momentum transfer becomes smaller or more tightly bound inner-shell electrons are considered, the impulse approximation is no longer valid. In this case the cross section is a rather complicated function of the initial and final states, polarization and the momentum transfer and the Compton profile can no longer be factorized out. There have been numerous theoretical approaches to this problem; an extensive review has recently been given by Kane [2]. Briefly speaking, the momentum transfer can be related to a dimensionless quantity, ka, where k is the length of the scattering vector and a the Bohr radius of the orbital in question. When $ka \gg 1$, the IA should be valid; on the other hand

0953-8984/96/132153+10$19.50

$ka \ll 1$ leads usually in metals to the collective electronic excitations [3]. The intermediate region $ka \simeq 1$ is the area of interest in this work, even though the tightly bound inner-shell electrons do not generally contribute significantly to the solid-state properties of matter. The motivation to understand the behaviour of the inner-shell electrons arises mainly from the wish to be able to reliably subtract them off from the total Compton profile in order to study the generally more interesting valence electrons.

Experimentally there are two basic ways to study the cross section of inelastic scattering from tightly bound electrons. (i) The first is to measure the total cross section including all of the electrons and then separate the inner-shell contribution [4, 5, 6]. This is a difficult task because the major contribution of the scattered spectrum has its origin in the loosely bound outer electrons and the subtraction of the minor part is complicated by the effects of background, multiple photon scattering and bremsstrahlung produced by the photoelectrons and Compton electrons. (ii) The second is to use a technique where the scattered photon is detected in coincidence with the fluorescence photon created when the inner-shell hole left by the Compton electron is filled. In this case the desired electron shell can be studied separately, but the counting rate is very low because of the low probability of detecting two photons simultaneously with two separate detectors. Almost all of these studies have been done using γ-ray sources; the incident-photon energies extend from 60 keV (^{241}Am) to 1.1 MeV (^{65}Zn). In order to have a well-defined momentum transfer only a small part of the scattered radiation can be used, which leads to extremely long measuring times even if high-activity sources are used. It should also be mentioned that an alternative coincidence technique, so-called (e, 2e) spectroscopy, has been successfully applied to study the electron momentum distributions of bound electrons [7]. This method is particularly useful for studying atoms or molecules, but the use of an electron beam instead of high-energy photons is more problematic if bulk electronic properties of solids are considered.

Bright and intensive synchrotron radiation has opened up new possibilities in the study of weak-scattering processes suffering from low counting rates. For the coincidence experiments this solution is not so obvious. As pointed out by Marchetti and Franck [8] and Hämäläinen *et al* [9] the problems due to the pulsed source make the random coincidence rate extremely high compared with that for a continuous source, especially when the number of the electron bunches in the storage ring is small.

In this work we present a new experimental solution for improving the coincidence counting statistics and the momentum resolution. Focused and monochromatized characteristic Kα_1 x-rays from a tungsten anode tube are used instead of a gamma-ray source. The photon energy, 59.32 keV, is very close to that obtained from a ^{241}Am source but due to the focusing x-ray optics the problems related to the large beam divergences can be avoided. The second improvement is that of using a modified fast–slow coincidence technique with simultaneous random coincidence detection to improve the signal-to-background ratio.

2. Experiment

For the 60 keV incident energy, Cu offers an excellent opportunity to study the intermediate-momentum-transfer range. For the three different scattering angles of 90°, 115° and 140° used in this experiment, the parameter ka discussed before takes the values 0.74, 0.86 and 0.94 at the Compton peak, respectively. In order to study the K-shell contribution to the inelastic scattering the Cu K fluorescence was detected in coincidence with the scattered photon. In the case of Cu these fluorescence energies are high enough to give good timing signals but low enough not to lead to overlap with the Compton profile.

The sample used in these studies was a thin copper foil. Because the mean free path

for the Cu K fluorescence ($1/\mu = 22$ μm) is much lower than for the scattered radiation, the useful thickness of the sample foil is determined by the fluorescence absorption. A foil having a thickness of 17 μm was therefore selected. The measurement geometry was also chosen so that the fluorescence was measured at an angle close to the surface normal to reduce the absorption, and the incident beam was aligned to hit the sample at very much a glancing angle to increase the radiated volume and thus the counting rate.

The x-ray source is based on a W-anode x-ray tube operated in this work at the voltage of 150 kV and current of 3.8 mA [10]. The W Kα_1 radiation was separated from the continuous x-ray spectrum using a bent Ge(400) monochromator in a symmetric reflection geometry. The flux at the focus (15 mm high and 0.5 mm wide at the sample position) was calculated using both the measured elastic and Cu K-fluorescence-line intensities. The same scattering geometry as in the actual coincidence experiments was used in the flux determination to guarantee that most of the systematic errors like uncertainties in the solid angles, seen by the detectors, cancel out in the final results. The monochromatic photon flux turned out to be $(2.83 \pm 0.07) \times 10^6$ photons s^{-1} corresponding to 3.8×10^5 photons s^{-1} mm^{-2}, which is a factor of three more than obtained from a 1 Ci ^{241}Am γ-ray source in similar geometrical conditions. The real improvement, however, is that the compact beam size allows better positioning of the detectors and shielding which reduce the random and false coincidence events. The best obtainable total momentum resolution of the spectrometer is 0.53 au (FWHM) which includes the contributions from the incident beam energy width (the natural width of the W Kα_1 line is 45 eV) and the resolution of the Ge detector which was used to measure the scattered photons. However, since the K-shell electrons are well localized in r-space, their momentum distribution is very broad and no especially high momentum resolution was needed for this work. Therefore, the momentum resolution was compromised to gain higher counting rates by placing the detectors as close as possible to the sample. In this case the momentum resolution is dominated by the uncertainty of the scattering angle and was 1.25 au for a scattering angle of 140°, for example. This also includes the contribution from the Ge detector energy resolution (400 eV at 60 keV).

The K-shell contribution to the Compton scattering cross section was separated by detecting in coincidence the fluorescence photon following the refilling of the intermediate K-shell hole. The fluorescence radiation from a polycrystalline sample is isotropic, and thus no angular resolution is needed for the fluorescence detection. However, a solid angle as large as possible is essential. Even if the Compton scattered photon from the K shell were to hit the Ge detector, the event would be missed unless the subsequent fluorescence photon reached the fluorescence detector. The probability of observing the fluorescence photon is simply proportional to the solid angle of the fluorescence detector (reduced by the absorption effects). Moreover, only a proportion of the holes are filled radiatively. In the case of Cu, for example, as many as half of the K-shell holes are filled through non-radiative channels, and thus increase the random coincidence counting rates. This is due to the fact that even though a scattered photon from the K shell is detected, there is no corresponding fluorescence photon to be observed.

Also, the energy resolution of the fluorescence detector needs only be good enough to separate the fluorescence lines from the background and from the Compton scattering contribution. Therefore, a NaI scintillation counter (with a diameter of 2″) was used to detect the Cu K-fluorescence photons. Both Kα and Kβ components were included within the accepted energy window since both lines indicate the same intermediate electron hole on the K shell. The detectors were placed on opposite sides of the sample foil (see figure 1) and the sample–detector distances were 67 mm (NaI) and 51 mm (Ge), corresponding to solid angles of 0.35 sr (2.8% of 4π) and 3.8×10^{-2} sr, respectively. Carefully designed

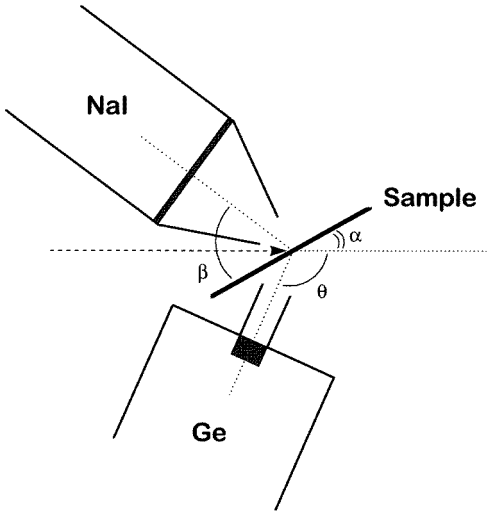

Figure 1. A schematic picture of the set-up of the detectors and lead shielding during the experiment (not to scale). The angles α (incident W Kα_1 radiation) and β (fluorescence radiation), taken relative to the plane of the sample, were typically $\alpha \approx 20^\circ$ and $\beta \approx 55^\circ$.

lead collimators were placed in front of both detectors to prevent any direct scattering from one detector to another. This is crucial because the process of Compton scattering off the scintillation counter can mimic the Cu fluorescence. In this case the energy of the Compton electron left in the detector after a scattering process can be within the fluorescence energy window. If the scattered photon is seen by the Ge detector, a false coincidence event is registered. Our focused x-ray beam made it possible to use very short sample–detector distances and thus maximize the solid angles seen by both of the detectors without risk of detector–detector scattering.

The modified fast–slow coincidence set-up was operating as follows. The timing signals from both detectors were first processed in the timing filter amplifiers to improve the rise-time characteristics and the signal-to-noise ratio of the pulses. Constant-fraction discriminators operating in ARC mode (=amplitude rise-time compensated) were used in both counting chains to give the time reference signals. The time difference between two simultaneous signals in the different detectors was then adjusted to be well above zero using a nanosecond delay unit. Next, the time difference between the two signals was converted into a voltage using a time-to-amplitude converter (TAC). In the slow part of the circuit a fast single-channel analyser was used to pick up signals corresponding to the Cu-fluorescence photons from the scintillation counter spectrum. This information was then processed by the TAC giving an output signal only when both the time and the energy conditions were satisfied. This signal was then used to gate the measured Compton spectrum from the Ge detector.

On the basis of the TAC time difference spectrum a total time resolution of 24 ns (FWHM) was obtained. The time window for two simultaneous events was set to be 43 ns. A measuring period of 500 000 s was used for each scattering angle. However, the total measurement time was divided into shorter periods in order to monitor the stability of the system. The integrated counting rates were 80 cps (Ge Compton detector, 10–65 keV) and 1400 cps (NaI fluorescence detector, 4–11 keV) at the scattering angle of

115°, for example. The corresponding integrated counting rate in the coincidence mode was 0.024 cps within the energy window of 10–65 keV. In addition to the true desired coincidence events there are other coinciding processes which can be divided into random and false coincidences. A simultaneous but accidental observation of an inelastically scattered photon and a K-fluorescence photon can take place if the inelastic scattering event and a fluorescence detection following (i) an independent photoabsorption process or (ii) an independent inelastic scattering process take place within the time window. This random (or chance) coincidence contribution can be measured and then subtracted by delaying the signal from one counting chain in such a way that the true coincidences no longer give any contribution. A delay of 48 ns was used in this work. In the present work both the true and the random coincidence spectra were measured simultaneously using two separate multichannel analyser cards. This is essential for improving the signal-to-noise ratio if there are any time-dependent instabilities in the system. In the delayed time window of 43 ns the integrated random coincidence counting rate of 0.008 cps was obtained. This corresponds to a 33% contribution to the total counting rate of 0.024 cps, significantly less than in the previous synchrotron experiment (95%) [8] and about the same as in the previous γ-ray experiment (25%) [11].

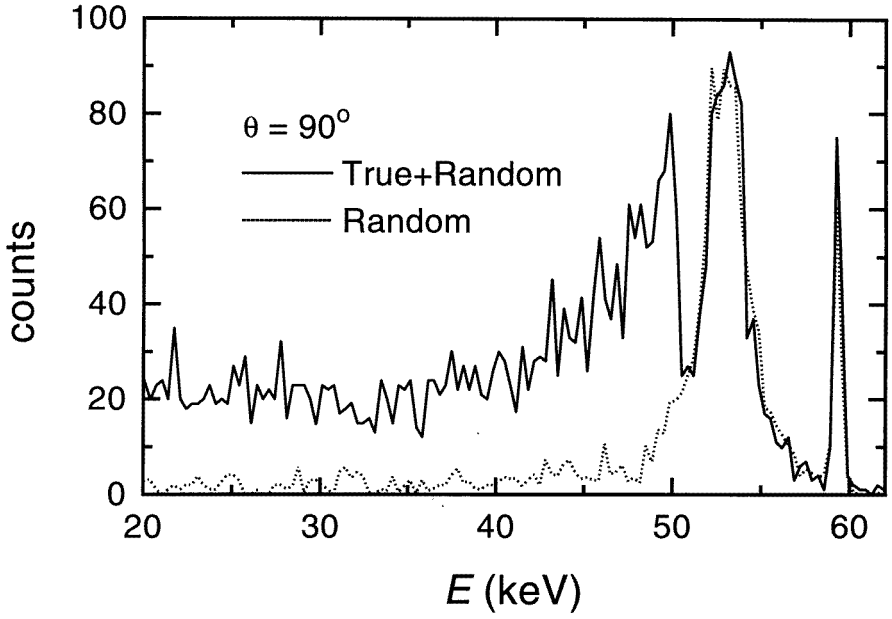

Figure 2. Raw data at the scattering angle of 90°. The measured random coincidence spectrum is also shown in the figure. The total measurement time was 250 000 s.

Figure 2 shows an unprocessed measured energy spectrum using a scattering angle of 90°. Because the Compton shift at this geometry is small (6.2 keV), a separate K-shell contribution can be seen apart from the random coincidence spectrum. A time-delayed random coincidence spectrum is also shown for comparison and this clearly demonstrates the success in measuring the random coincidences: the contribution above the K edge is fully reproduced. The experimental results were corrected for these random coincidence events by simple subtraction. The random/true coincidence ratios (given in counts s^{-1} in

the energy window of 10–65 keV) were 0.006/0.020, 0.008/0.024 and 0.010/0.030 for the scattering angles of 90°, 115° and 140°, respectively. However, it should be noticed that at low energies the detected counts are almost all true events.

The measured count rate n is related to the scattering cross section according to the equation [12]

$$n = n_0 \frac{\mathrm{d}^2\sigma}{\mathrm{d}E_2\ \mathrm{d}\Omega_{sc}} \Delta E_2\, \Delta\Omega_{sc} \frac{\rho}{\sin\alpha}\, \frac{\omega_K}{4\pi}\, \Delta\Omega_f\, \frac{\mathrm{e}^{-\mu_{sc}d/\sin(\theta+\alpha)} - \mathrm{e}^{-\mu_1 d/\sin\alpha - \mu_f d/\sin\beta}}{\mu_1/\sin\alpha + \mu_f/\sin\beta - \mu_{sc}/\sin(\theta+\alpha)}\, \epsilon_{sc}\epsilon_f \tag{2}$$

where n_0 is the incident photon flux (cps), ΔE_2 the MCA energy channel width (keV), $\Delta\Omega_{sc}$ and $\Delta\Omega_f$ the solid angles (sr) for the scattered and fluorescence photon detectors, respectively, ρ the density (g cm^{-3}) and d the thickness (cm) of the sample, μ_1, μ_{sc} and μ_f the linear absorption coefficients (1 cm^{-1}) for the incident, scattered and fluorescence energies, respectively, α and β the incidence and exit angles relative to sample surface for incident and fluorescence radiation and θ the scattering angle, ω_K the fluorescence yield, and ϵ_{sc} and ϵ_f the efficiencies of the scattered and fluorescence photon detectors. These efficiencies include the energy-dependent corrections for the detector window and air path absorption. The scattering cross section is given in units of cm^2 g^{-1} keV^{-1} sr^{-1}. This can be transformed to b keV^{-1} sr^{-1}/atom by multiplying the cross section by $0.6022/M$ where M is the molar mass (g mol^{-1}). Equation (2.1) includes the absorption effects and assumes that the fluorescence radiation is measured on the same side of the sample as the incident beam and the scattered spectrum is measured in transmission. Also, the solid angles and the energy width of the MCA are assumed to be small enough that the cross section is approximately constant within these ranges.

Figure 3 shows the absolute experimental cross sections for three different angles. It can be seen that there is an additional angle-independent contribution in the measured spectra at low energies which is clearly not due to the Compton scattering from 1s electrons. The origin of this low-energy tail is the bremsstrahlung produced by the photoelectrons in the sample. This contribution is so pronounced because the photoelectric cross section at this energy is still more than one order of magnitude more than the inelastic cross section. It should be noticed that these events are detected as true coincidences since the K-shell fluorescence is created after the photoabsorption with the same probability as in the case of the inelastic scattering process from the K shell. Because the photoelectric absorption mainly takes place at the K shell, this contribution has the maximum energy of $\hbar\omega_1 - K_{bind} \approx 50.3$ keV and the energy dependence is proportional to $1/\hbar\omega_2$ [13]. A computational fit based on these arguments was calculated and this contribution was subtracted from the experimental data (see figure 3). The fact that the bremsstrahlung contribution is angle independent is a proof of its origin and that all of the angle-dependent corrections to the measured spectra have been successful.

The final results for the absolute inelastic scattering double-differential cross section of Cu K electrons at three different scattering angles are shown in figure 4. Due to use of a well-collimated beam from a continuous source it is possible now, for the first time, to make a quantitative analysis of the various cross section calculations at the x-ray energies. The previous gamma-ray results for Cu [11, 14] were not measured on an absolute scale or were additionally suffering from tricky false coincidence events [15]. The statistical accuracy in the only existing synchrotron experiment on Cu [8] was so low that it prevented us from reaching quantitative conclusions, although the absolute cross sections were determined.

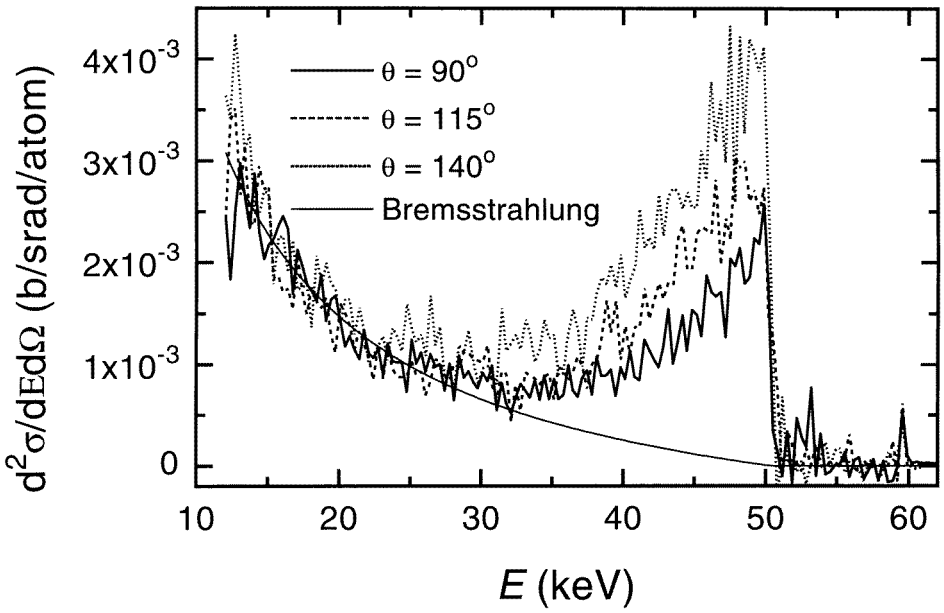

Figure 3. True coincidence spectra in absolute units for three scattering angles after the subtraction of the chance coincidence contribution and the absorption correction. The fitted bremsstrahlung contribution (BS) is also shown.

3. Results and discussion

Various approaches for calculating the inelastic scattering cross section for bound electrons, reviewed by Kane [2], end up in relativistic calculations by Holm [16], Holm and Ribberfors [17] and Bergstrom *et al* [18]. According to Holm [16] the Compton profile can be factorized from the measured cross section at large scattering angles (providing, of course that the experiment has been made in the region where $ka \geqslant 1$), and the accuracy is better on the high-energy side of the profile. At lower scattering angles and on the low-energy side the error is larger. The results of these calculations are also shown in figure 4. The overall agreement in all cases is surprisingly good, although there is a small but systematic difference that occurs in such a way that the experimental cross section is higher at low energies. In the case where $\theta = 90^\circ$, when only the low-energy tail of the K-shell contribution is obtained, the difference between the experiment and the theory is somewhat more pronounced. These observations can also be interpreted using the binding parameter ϵ/q where $\epsilon = \sqrt{2mE_{1s}}$ and q is the momentum transfer. According to Holm and Ribberfors [17] the error in the impulse approximation increases with increasing binding parameter, and the maximum deviation in per cent of $J(0)$, the Compton profile peak, is $10\epsilon/q$ for 1s electrons. In the present case the binding parameter varies between 1.2 and 1.4, i.e. the error when the impulse approximation is used is about 10% and is in agreement with our results. Compared with our previous nonabsolute coincidence experiment [11] where the measured data were normalized according to the IA, there is a close agreement; the significance of the present results is that no normalization is included.

Figure 5 shows the cross sections at three different angles transformed to the momentum scale using the standard cross section formula where the cross section is factorized. In this

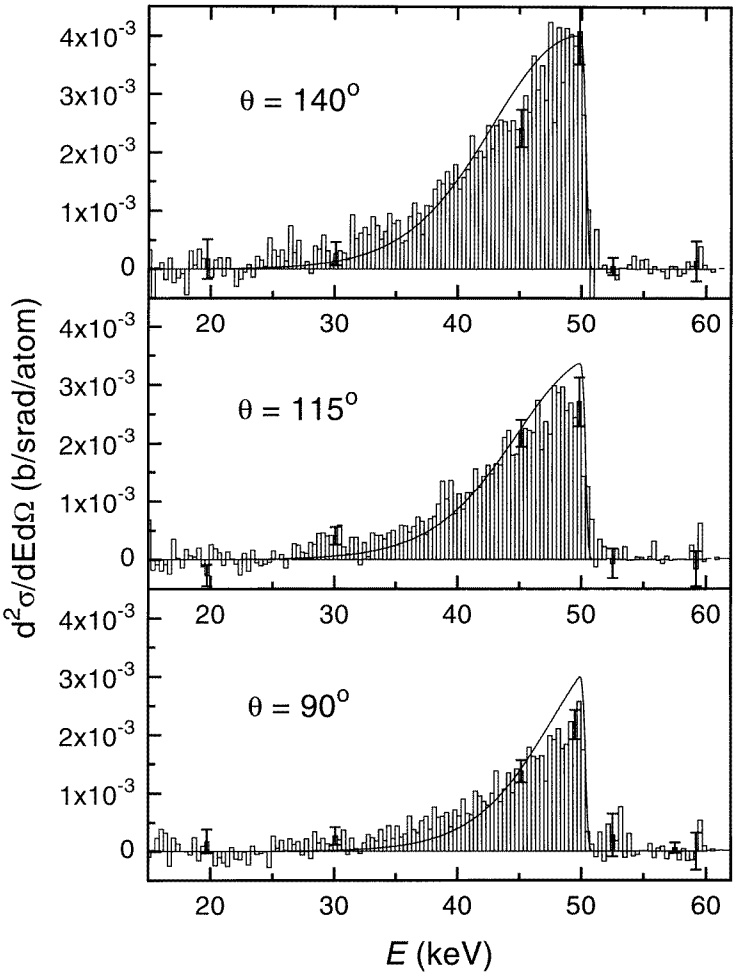

Figure 4. Experimental K-shell Compton scattering cross sections for three different scattering angles. The solid lines correspond to the numerical calculation based on Holm's theory [16]. The statistical error bars are shown at some points.

figure all three profiles look identical within the statistical accuracy except for the different cut-offs because of the different scattering angles and subsequent different Compton shifts. From this we can conclude that the deviation from the theory is more general in nature and does not significantly increase when we are further away from the backscattering geometry. Furthermore, the area of the Compton profile seems to be in surprisingly close agreement with the IA result. The experimental area is about 10% higher than one would expect on the basis of the simple normalization according to number of electrons. This extra contribution is due to the low-energy tail as discussed earlier in the text.

Another relativistic approach to the inelastic scattering cross section has been described by Bergstrom *et al* [18] using a relativistic second-order S-matrix calculation within the independent-particle approximation. They conclude that the crucial parameter for fulfilling the impulse approximation is P_{av}/k where $P_{av} = \sqrt{p_z^2 + 2\langle p^2\rangle/3}$, and $\langle p^2\rangle$ is the expectation value of the square of the momentum for the initial bound electron state

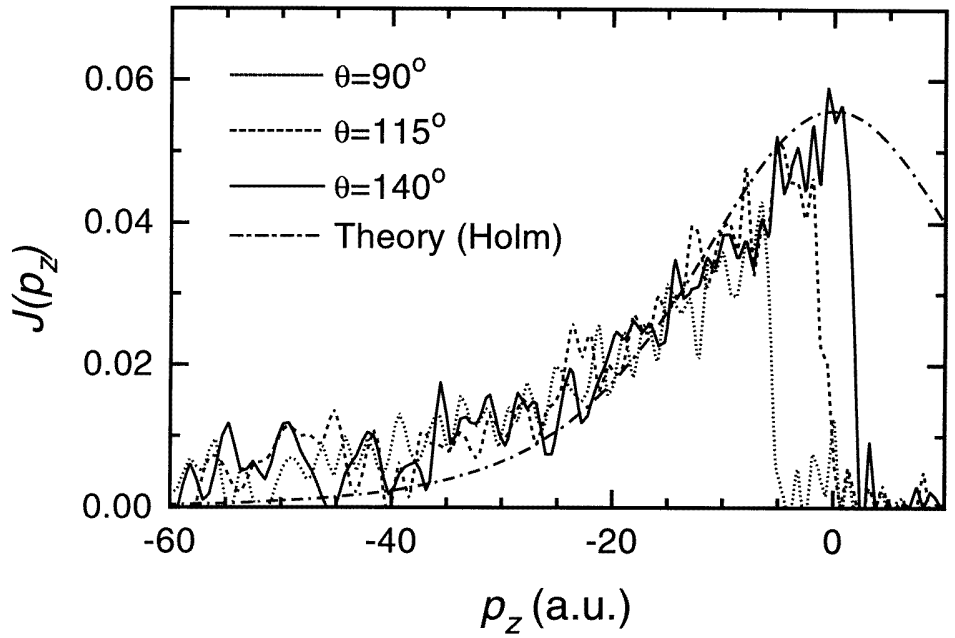

Figure 5. The experimental cross sections transferred to the momentum scale. The solid line corresponds to Holm's theory [16] (1 au = 1.99×10^{-24} kg m s^{-1}).

and k is the magnitude of the momentum transfer, i.e. closely related to the parameter given by Holm and Ribberfors [17] but taking properly into account the average momentum that contributes to a given part of the scattered spectrum. In our experiment this parameter varies between 0.60 and 0.77 at the Compton peak. When $P_{av} \leqslant 1$ the impulse approximation should work and in this momentum range the two calculations [16, 18] give almost identical results. The basic difference arises when the soft photon part of the scattered spectrum is considered. A low-energy tail, higher than predicted by the impulse approximation, is finally leading to the infrared divergence at very low energies.

Compared with the *S*-matrix calculation [18] our results show the same additional low-energy tail features compared with the impulse approximation at the energies below 40 keV. Unfortunately no numerical values, based on the *S*-matrix calculations, were available. Because of the large bremsstrahlung contribution no confirmation regarding the infrared divergence can be achieved on the basis of these results. An extremely thin sample and a windowless detector in the same vacuum chamber should be used to study this fundamentally interesting effect.

It should be noted that the accuracy of the impulse approximation has also been studied by looking at the asymmetry of the Compton profile or the shift of the peak maximum [19]. This so-called Compton defect has also been found experimentally but in the present case the resolution is too poor for any comparison with the calculations to be made.

In terms of the Compton profile experiments the present results are particularly useful because the high-resolution spectrometers used in the third-generation synchrotron sources operate in the energy region of 50 keV [20, 21]. In order to fully utilize the improved statistical accuracy the contribution of the inner-shell electrons should be accurately known before firm conclusions about the interesting valence electron states can be drawn.

Fortunately, it seems to be that, even in the extreme cases where the binding edge cut-offs are present in the experimental data, this contribution can be treated properly. Usually these cut-offs can be avoided by making a proper choice of the primary energy and the scattering angle; the accuracy of the IA is then, of course, better.

Finally it should be mentioned that despite the great success of the synchrotron radiation in the field of inelastic scattering experiments, coincidence studies still favour conventional sources. First experiments at the European Synchrotron Radiation Facility (ESRF) show [22] that although there can be as many as 990 electron bunches distributed in the storage ring, the true-to-chance ratio of coincidences is not better than 50%. Additionally, this optimized result was obtained using a primary photon flux four decades below the full power of the beam to reduce the random coincidence rate.

Acknowledgment

The authors are indebted to the Finnish Academy for financial support (Contract No 8582).

References

[1] Eisenberger P and Platzman P M 1970 *Phys. Rev.* A **2** 415
[2] Kane P P 1992 *Phys. Rep.* **218** 67
[3] Schülke W and Nagasawa H 1984 *Nucl. Instrum. Methods* **222** 203
[4] Pattison P and Schneider J R 1979 *J. Phys. B: At. Mol. Phys.* **12** 4013
[5] Reineking A, Wenskus R, Baumann A, Schaupp D, Rullhusen P, Smend F and Schumacher M 1983 *Phys. Lett.* **95A** 29
[6] Manninen S, Hämäläinen K, Schneider J R, Rollason A J and Drube W 1990 *Nucl. Instrum. Methods* A **290** 242
[7] McCarthy I E and Weigold E 1991 *Rep. Prog. Phys.* **54** 789
[8] Marchetti W and Franck C 1987 *Phys. Rev. Lett.* **59** 1557
[9] Hämäläinen K, Manninen S and Schneider J R 1990 *Nucl. Instrum. Methods* A **297** 526
[10] Manninen S, Honkimäki V and Suortti P 1992 *J. Appl. Crystallogr.* **25** 268
[11] Manninen S, Hämäläinen K and Graeffe J 1990 *Phys. Rev.* B **41** 1224
[12] Marchetti W and Franck C 1988 *Rev. Sci. Instrum.* **59** 407
[13] Evans R D 1955 *The Atomic Nucleus* (New York: McGraw-Hill)
[14] Namikawa K and Hosoya S 1984 *Phys. Rev. Lett.* **53** 1606
[15] Manninen S 1987 *Phys. Rev. Lett.* **53** 1500
This gives a discussion concerning the effect of detector–detector scattering of the coincidence spectrum.
[16] Holm P 1988 *Phys. Rev.* A **37** 3706
[17] Holm P and Ribberfors R 1989 *Phys. Rev.* A **40** 6251
[18] Bergstrom P M Jr, Suric T, Pisk K and Pratt R H 1993 *Phys. Rev.* B **48** 1134
[19] Gasser F and Taward C 1983 *Phys. Rev.* A **27** 117
[20] Sakurai Y, Tanaka Y, Bansil A, Kaprzyk S, Stewart A T, Nagashima Y, Hyodo T, Qanao S, Kawata H and Shiotani N 1995 *Phys. Rev. Lett.* **74** 2252
[21] Manninen S, Honkimäki V, Hämäläinen K, Laukkanen J, Blaas C, Redinger J, McCarthy J and Suortti P 1996 *Phys. Rev.* B **53** at press
[22] Hämäläinen K, Laukkanen J, Manninen S and Honkimäki V 1996 to be published